CHEMISTRY OF MATERIALS

pubs.acs.org/cm

Article

Relationship of the Molecular Structure and Transport Properties of Imide-Based Lithium Salts of "Acetonitrile/Water-in-Salt" Electrolytes

Xinyi Liu, Shao-Chun Lee, Soenke Seifert, Randall E. Winans, Y Z,* and Tao Li*

Cite This: *Chem. Mater.* 2023, 35, 6415−6422

Read Online

ACCESS | Metrics & More | Article Recommendations | Supporting Information

ABSTRACT: "Water-in-salt" (WIS) electrolytes exhibit excellent safety and electrochemical performance. However, they possess high concentrations, relatively low diffusion coefficient, and high viscosity. "Acetonitrile/water in salt" (AWIS) electrolytes can overcome the disadvantages of WIS electrolytes. Under relatively low concentrations, AWIS electrolytes show good electrochemical performance comparable to WIS electrolytes and low conductivity. Herein, we investigate the relationship between the solvation structures and the transport properties using small-angle X-ray scattering and molecular dynamics simulation. We observed two solvation behaviors of AWIS: anions dissolved in acetonitrile forming small acetonitrile/anion clusters and additional water further dissolving the small acetonitrile/anion clusters. The introduction of acetonitrile weakens the water−solute interaction and enhances the cation−anion interaction, which results in an enhanced dynamical slowdown as the concentration increases. This work provides molecular-level understanding of the connection between two-stage solvation structures and transport properties for imide-based lithium salt solutions.

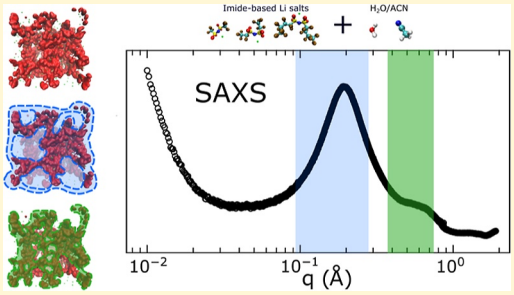

INTRODUCTION

The concentration of electrolytes dictates the performance of lithium-ion batteries (LIBs).[1−6] Yamada et al. discovered that electrolytes with high concentration have a substantially broader electrochemical stability window and a significantly improved oxidation potential, which are beneficial for forming a stable solid electrolyte interface.[2] Applying this strategy to aqueous LIBs, a new aqueous electrolyte called "water-in-salt" (WIS) containing 21 m (mol/kg) lithium bis(trifluoromethane sulfonyl)imide (LiTFSI) has been proposed by Suo et al.[7] This aqueous electrolyte has a wider electrochemical stability window (~3.0 V) and higher lithium ion de/intercalation potential. The solvation structures of dilute and WIS electrolytes differ significantly, revealed by the recent small-angle X-ray scattering (SAXS) investigation.[8−11] Two unique solvation structures, namely, $TFSI^-$-solvated structures and $TFSI^-$ networks, have been observed in the LiTFSI aqueous solutions. At the low concentration regime, only $TFSI^-$-solvated structures exist, while at the medium concentration regime, the two structures coexist. The $TFSI^-$ network is the only existing structure in the WIS electrolyte containing 21 m LiTFSI, which is the key to the enlarged electrochemical stability window. This solvation behavior could also be observed in other imide-based lithium salts. The transition between these two characteristic solvation structures was found to occur at ~20% of the salt volume fraction (f_{salt}), which is defined as the effective volumetric ratio between the salt and water.[9,12]

Because of the strong electrostatic cation−anion attraction in highly concentrated electrolytes, WIS electrolytes have relatively low conductivity and high viscosity, which causes the LIBs with WIS electrolytes to have a limited rate of performance.[13−19] On the other hand, the exceptionally high concentration of WIS electrolytes tends to result in salt precipitation, which inevitably limits the applicable temperature range of aqueous LIBs.[14,17] To overcome these problems, Dou et al. introduced a co-solvent-in-salt system by mixing acetonitrile (ACN) with a typical WIS electrolyte to create an "acetonitrile/water-in-salt" (AWIS) electrolyte.[20] Compared with the WIS electrolyte, the non-flammable AWIS electrolyte with 5 m shows improved conductivity, decreased viscosity, and lowered freezing point while maintaining a wide stability window (about 3.0 V).

It has been widely accepted that Li^+ ions are well solvated, while $TFSI^-$ remains relatively free in diluted LiTFSI acetonitrile solutions.[21,22] However, water molecules are bipolar and can effectively solvate both Li^+ and $TFSI^-$. Hence, the investigation of the solvation structures of AWIS and the relationship between them and the physical properties

Received: May 14, 2023
Revised: July 7, 2023
Published: August 2, 2023

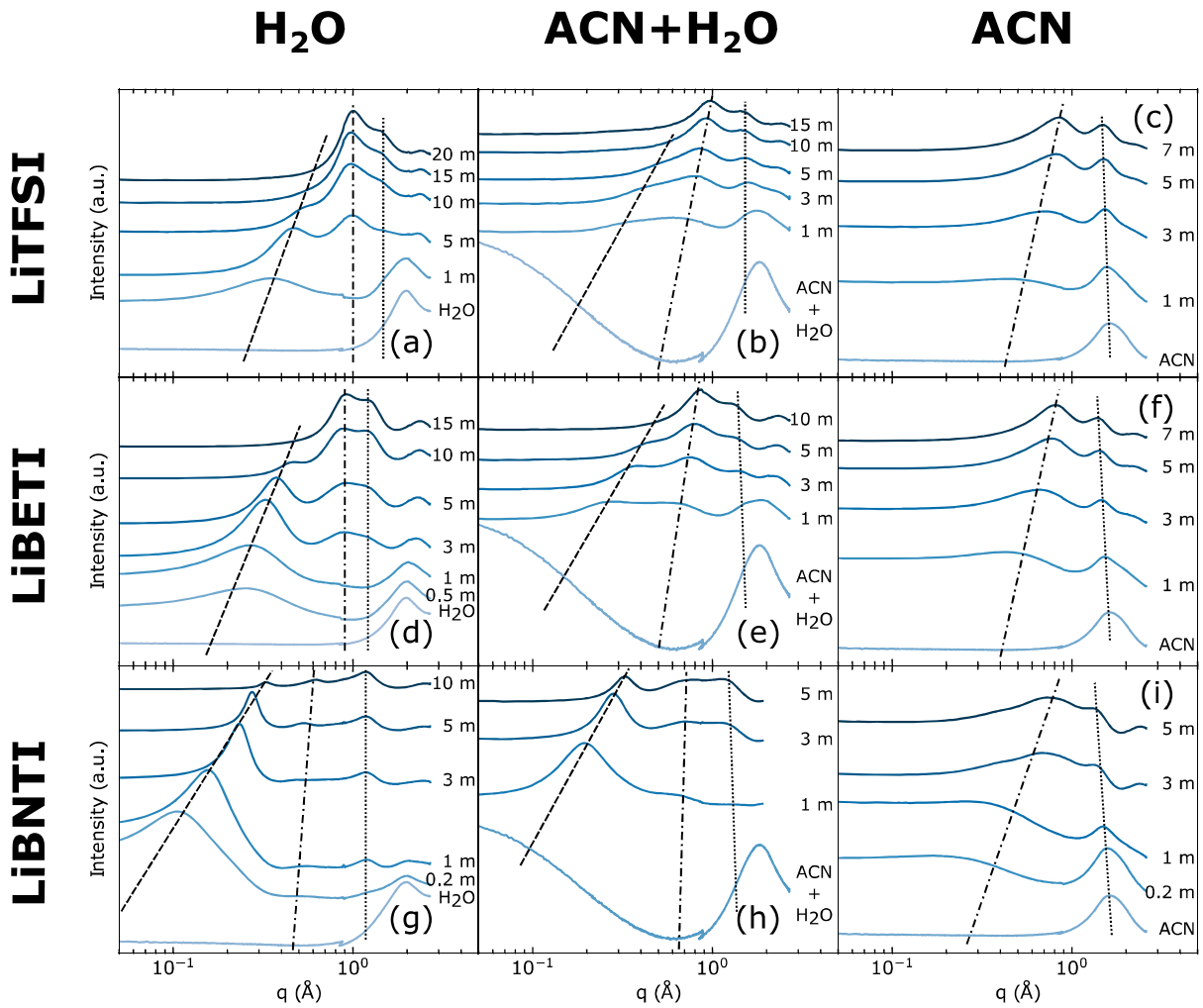

Figure 1. SAXS profiles of three imide-based lithium salt solutions. Solutes: (a–c) LiTFSI, (d–f) LiBETI, and (g–i) LiBNTI. Solvents: (a,d,g) H_2O, (b,e,h) ACN and H_2O, and (c,f,i) ACN. The data is offset for clarity. Both *x*- and *y*-axes are in the log scale. The peaks in the SAXS profiles are identified as peak a (dashed), peak b (dashed-dotted), and peak c (dotted).

such as viscosity and conductivity are attractive.[23] Pedro et al. employed molecular dynamics (MD) simulation to investigate the structural and dynamic properties of AWIS. They found that the addition of ACN to WIS electrolytes weakens the cation–anion interactions and decreases the coordination of ionic pairs in the mixtures.[23] In addition, because of the breakdown of the strong electrostatic cation–anion interaction network, the diffusion of species increases in the AWIS electrolytes. So far, most results in the literature on the solvated structures and dynamics properties of WIS electrolytes are focused on the high concentration (~20 m) regime and only one lithium salt LiTFSI.[10,12,18,24−31] However, the fundamental understanding of the structure/property relationship of AWIS is still limited.[23]

In this work, we combined SAXS with MD simulation to investigate the solvation structures, viscosity, and diffusion coefficients of three imide-based symmetric lithium salts, LiTFSI, lithium bis(pentafluoroethane sulfonyl)imide (LiBETI), and lithium bis(nonafluorobutane sulfonyl)imide (LiBNTI) aqueous, ACN, and ACN/water (mixture solvent) solutions systematically from low to high concentrations. From the SAXS measurements, we found that only relatively low concentrations were required to form the anion networks when the three imide-based lithium salts were dissolved in the mixture of acetonitrile and water. More interestingly, the peaks at the low *q* region are only from water. In contrast, the peaks at the middle *q* region are caused by both water and acetonitrile, which form the panorama view that acetonitrile dissolves anions to form small acetonitrile/anions clusters, and water further dissolves the small acetonitrile/anions clusters. The addition of acetonitrile weakens the interaction between the solvent and anion while the interaction between the cation and anion is enhanced, which leads to a more "rigid" ionic network. We conclude that this increase in rigidity of the ionic networks is the root cause of a more drastic dynamical slowdown as the concentration increases. Moreover, in the end of this paper, we also try to answer several critical questions which are (1) why does the AWIS electrolyte show comparable electrochemical properties with the WIS electrolyte at a relatively low concentration? (2) What are the solvation structures of AWIS electrolytes and what are the roles of water and acetonitrile? (3) How do the molecular structures affect the viscosity and diffusion coefficients? (4) If the three imide-based lithium salts show the same phenomenon?

RESULTS

To fully understand the solvation structure, we measured the SAXS profiles of LiTFSI, LiBETI, and LiBNTI salts in water,

https://doi.org/10.1021/acs.chemmater.3c01148
Chem. Mater. 2023, 35, 6415−6422

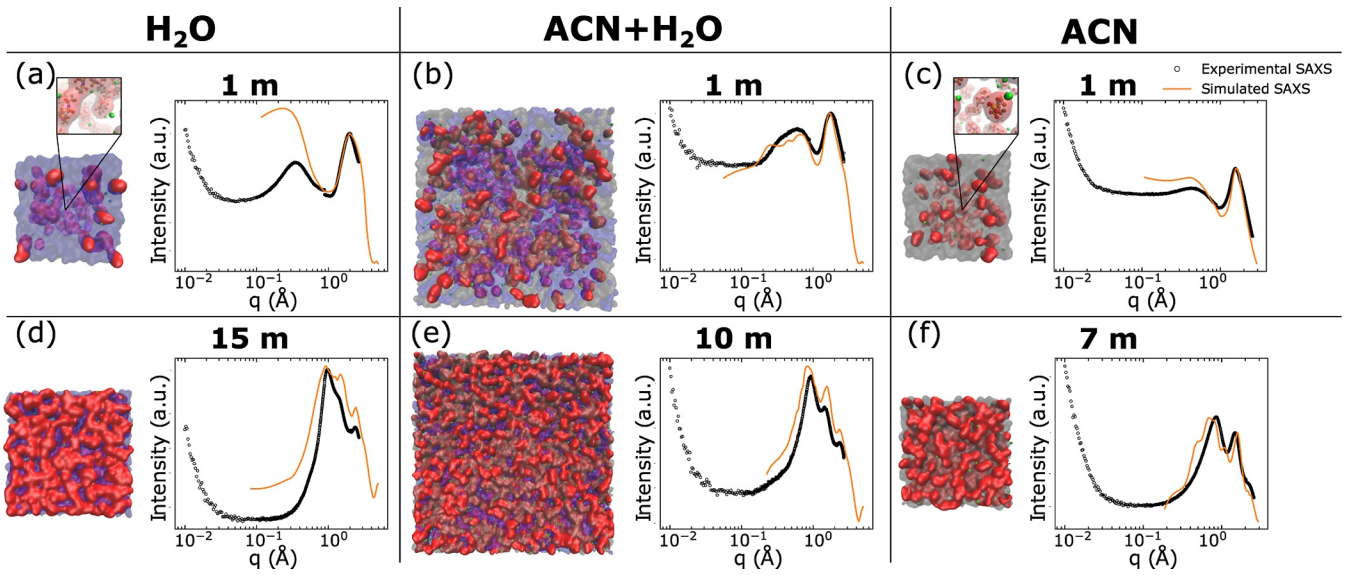

Figure 2. MD snapshots and comparisons between the experimental (black circles) and simulated (orange lines) SAXS profiles of LiTFSI aqueous solutions at low concentrations (a–c) and high concentrations (d–f).

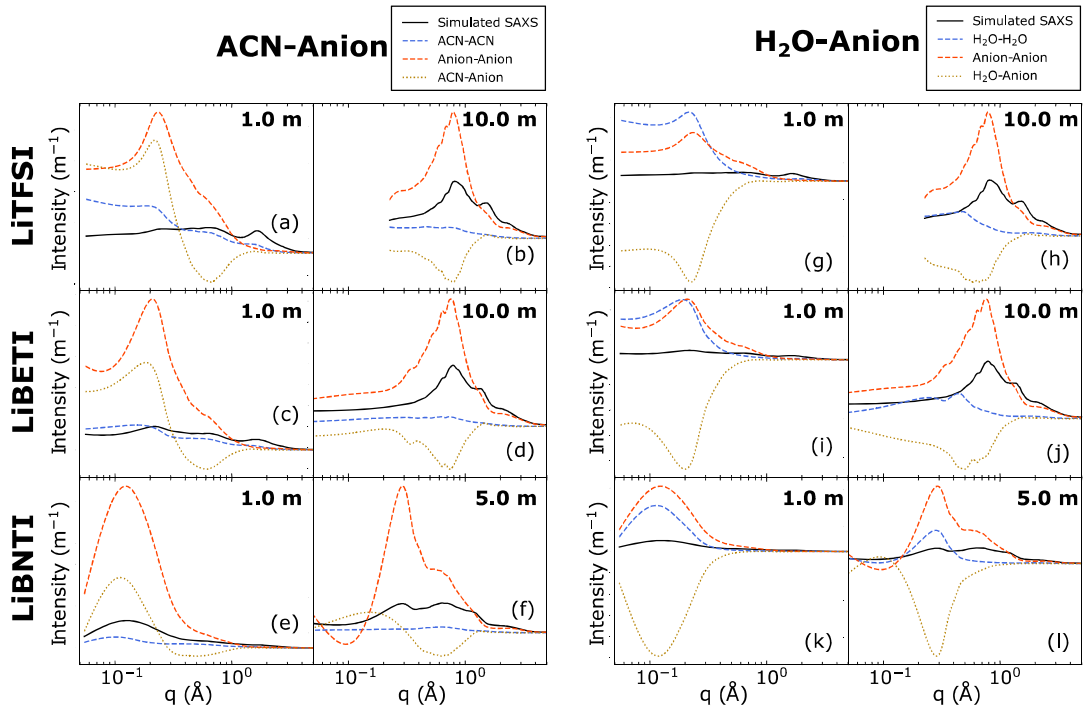

Figure 3. Decomposition of the simulated SAXS profiles for ACN and H_2O mixture systems. (a–f) Correlations between ACN and the anion and (g–l) correlations between H_2O and the anion. (Black solid lines: the simulated SAXS profiles; blue dashed lines: solvent–solvent self-correlations; red dashed lines: anion–anion self-correlations; and yellow dotted lines: solvent–anion cross-correlations).

water–acetonitrile mixture, and acetonitrile with a systematic variation of concentration, as shown in Figure 1. We observed three peaks in these aqueous solutions labeled peak a, b, and c. Peak a shifts to a higher q with a decreased intensity as the concentration increases; peak b remains at a similar peak position with increased intensity as the concentration increases. According to the analysis of the simulated SAXS profiles in our previous study,[9] peak a is primarily contributed by the anion clusters and water channels which compensate one another at the nanometer scale, peak b is primarily contributed by the interaction of the neighboring anions, which are bridged by the cations (charge ordering) and the water molecules, indicating the structures of anion networks, and peak c is primarily contributed by the correlations of fluorocarbon chains between neighbor anions. In the case of ACN solutions, there are two observable peaks. The peak at the lower q range shifts to higher q as the concentration increases. Since this peak has a q range closer to peak b in aqueous solutions, we labeled it peak b. Furthermore, it has been well established that the cations are well solvated, while the anions remain relatively free in the diluted organic electrolytes, indicating that the peak at the lower q region does not correspond to anion clusters described by peak a in aqueous solutions.[21]

https://doi.org/10.1021/acs.chemmater.3c01148
Chem. Mater. 2023, 35, 6415–6422

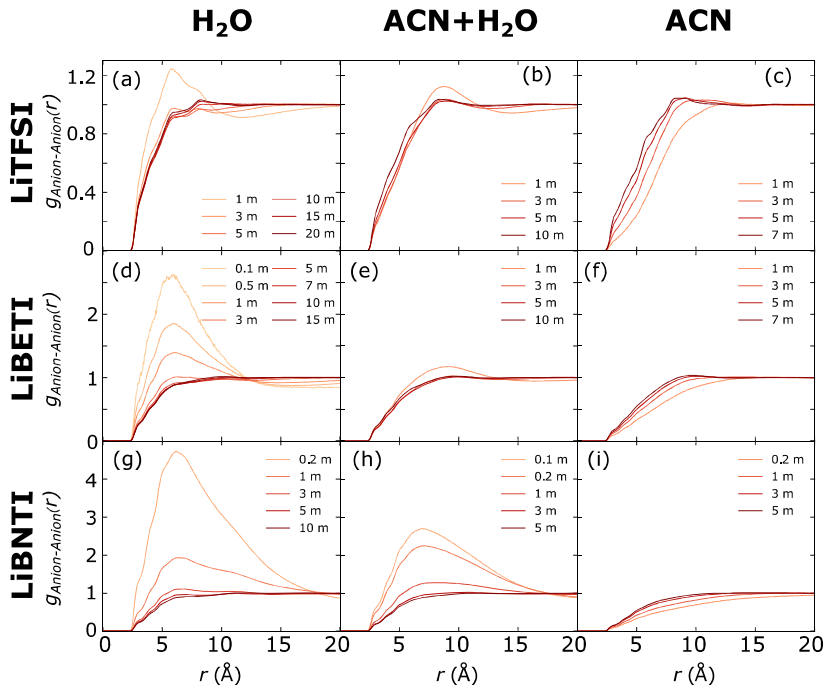

Figure 4. Anion−anion partial PDFs of the aqueous solutions in this study. Solutes: (a−c) LiTFSI, (d−f) LiBETI, and (g−i) LiBNTI. Solvents: (a,d,g) H_2O, (b,e,h) ACN and H_2O, and (c,f,i) ACN.

As for the mixture solutions, we found three peaks that were similar to our observation in the aqueous solutions. We labeled the three peaks peak a, b, and c, as they showed similar trends as peaks a and b in the aqueous solutions upon increasing concentration: (1) peak a shifts to higher q; (2) the peak a intensity decreases, while the peak b and c intensity increases. On the other hand, we discovered two observable differences from the aqueous solutions: (1) the ratio of peak a to peak b intensity is lower in mixed solvent solutions than in aqueous solutions. For LiTFSI in particular, the reduced peak a-to-peak b ratio makes peak a appear as a shoulder instead of a separate peak. (2) Unlike peak b position in aqueous solutions, the peak b position in mixture solvent solutions shows an observable left shift as the concentration increases. We suspect that this left shift originates from peak b in acetonitrile solutions. Figure S1 shows the corresponding d spacing from peak a and peak b positions, namely, $d = 2\pi/q$. The concentration dependence of the d spacing of peak a shows a minor difference between aqueous solutions and mixture solvent solutions. On the other hand, the d spacing of peak b shows a stronger concentration dependence as the system contains more acetonitrile, suggesting that the corresponding structure of peak b in the mixture solvent solutions is a combination of the structures associated with peak b from aqueous solutions and acetonitrile solutions.

To confirm our hypothesis, we performed MD simulation. Figure 2 depicts the MD snapshots and the comparisons between the experimental and simulated SAXS profiles of LiTFSI in three different solvents at both low and high concentrations (snapshots of LiBETI and LiBNTI solutions are illustrated in Figures S2 and S3). The size of the snapshots reflects the size of the simulation boxes. The simulated SAXS profiles for all the concentrations are plotted in Figure S4. The snapshots show that the regions occupied by the anions (red) are bulky in aqueous solutions and dispersed in acetonitrile solutions. The former corresponds to anion clusters, while the latter corresponds to individual anions. For the mixture systems, the anion clusters are still observable at 1 m, but a substantial number of individual anions is also observable.

To further understand the structural details, we decomposed the simulated SAXS profiles and examined the correlations between different subcomponents. We plotted the decomposition of the simulated SAXS for aqueous and acetonitrile solutions in Figures 3, S5, and S6. We found that peak a in aqueous solutions is composed of anion−anion and solvent−solvent self-correlations and a negative anion−solvent correlation as shown in Figure S5. This implies anion−solvent alternating structures; meanwhile, we also found that peak b of acetonitrile solutions implies the same anion−solvent alternation as shown in Figure S6. However, they do not correspond to the same length scales. Peak a in aqueous solutions corresponds to average length scales (d spacing) of 15, 20, and 38 Å for LiTFSI, LiBETI, and LiBNTI, respectively, while peak b in acetonitrile solutions corresponds to shorter length scales of 10 Å, 11 Å, and 18.3 Å for LiTFSI, LiBETI, and LiBNTI, respectively. Combined with our observation from MD snapshots, peak a in aqueous solutions is associated with the alternation between anion clusters and bulk water at the nanometer scale, while peak b in acetonitrile solutions is related to the alternation between individual anions (free anions) and ACN at the sub-nanometer scale.

Figure 3 shows the decomposition of the simulated SAXS profiles of the mixed solvent solutions. We grouped the decomposition into ACN−anion (Figure 3 left panel) and H_2O−anion (Figure 3, right panel) correlations. From the data at 1 m, we found that peak a (0.1−0.3 $Å^{-1}$) is composed of an anion−anion peak, a H_2O−H_2O peak, an ACN−ACN peak, and an ACN−anion peak but a H_2O−anion anti-peak. The destructive H_2O−anion signal suggests a compensating structure between bulk water and anion clusters which is identical to what we have discovered in the aqueous solutions. In contrast, the ACN−anion peak implies a homogeneous

https://doi.org/10.1021/acs.chemmater.3c01148
Chem. Mater. 2023, 35, 6415−6422

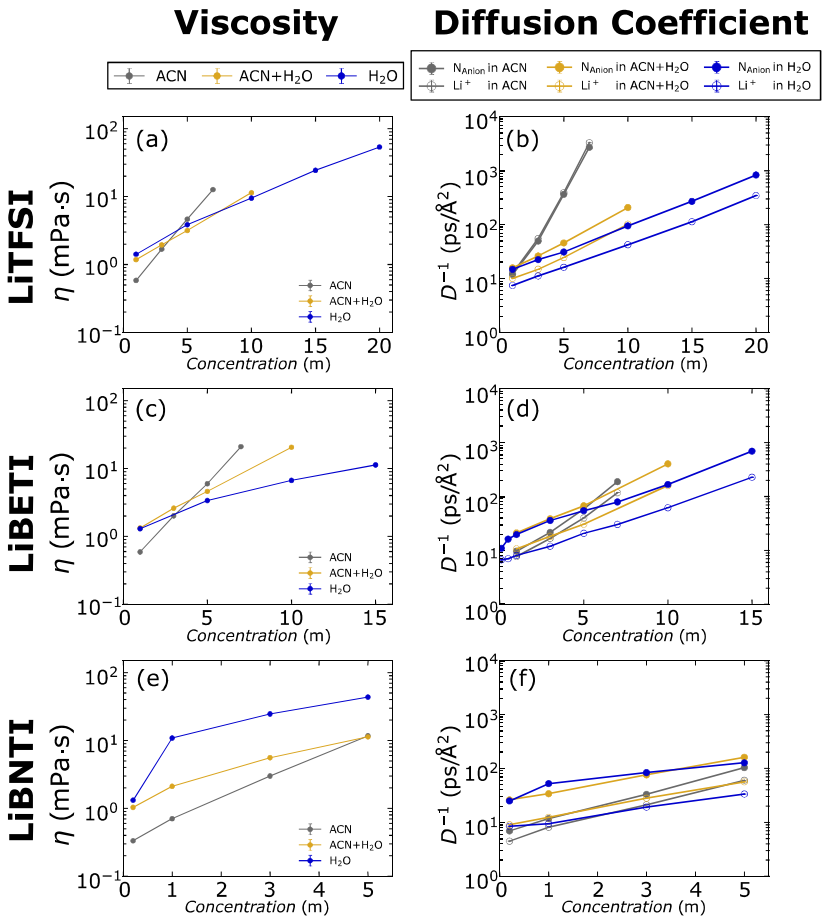

Figure 5. Experimental viscosities (a,c,e) and simulated diffusion coefficients (b,d,f). (Solid circles: the diffusion coefficient for the N atom of the anions and the diffusion coefficient for the cations).

mixture between the acetonitrile molecules and anions at the nanometer scale. However, the 1 m data show an ACN−anion anti-peak at the position near peak b (0.4−0.6 $Å^{-1}$), indicating that the acetonitrile molecules and anions exhibit an alternating structure, except that this structure forms at a smaller length scale than the water−anion alternation does. As for the data at high concentrations (10 m for LiTFSI and LiBETI and 5 m for LiBNTI), we found that the ACN−anion and H_2O−anion anti-peaks at the q range around peak b indicates that both ACN and H_2O exhibit alternating structures with the anions at a similar length scale at high concentrations.

To further show that the solutes are "relatively free" in ACN and prone to forming clusters in water, the partial pair distribution functions (PDFs) between the anions were calculated from the MD trajectories and are shown in Figure 4. We found a prominent peak in aqueous solutions, and its height and width increase with longer fluorocarbon chains. The height of the main peak significantly decreases with the addition of acetonitrile for all the salts. This trend rationalizes the tendency to form anion clusters in a water-rich environment but free anions in an acetonitrile-rich environment. The main peak in the mixture solvent solutions is observed, suggesting that the anion clusters still exist, which is consistent with the observation of peak a in mixture solvent solutions in both SAXS profiles and MD snapshots.

It is believed that the solvation structure has significant impacts on the transport properties of the electrolyte solutions, which would ultimately affect the battery's performance. Figure 5 shows the concentration dependence of the experimentally measured viscosities η and simulated inverse diffusion coefficients D^{-1}. We found similar trends between η and D^{-1}. In LiTFSI and LiBETI solutions, both η and D^{-1} exhibit a linear concentration dependence under log scale and a stronger concentration dependence with more acetonitrile in the solutions. At concentrations ranging from 3 to 5 m, solvents with more acetonitrile have higher η, even though pure acetonitrile has a viscosity ~2.6 times lower than water. This turnover in the trend of transport properties suggests that the additional structures of the salts provide significantly different rates of a dynamical slowdown in different solvents. However, this effect is not obvious in LiBNTI solutions; in addition, LiBNTI solutions exhibit a non-linear concentration dependence in aqueous and mixture solvent systems.

To further understand how the salts lead to substantially distinct dynamical slowdown rates in different solvents, we investigated the coordination numbers of oxygens from anions around cations ($CN_{O(anion)}$), which could be considered a quantitative measure of cation−anion interactions, as shown in Figure S7. We found that the number of oxygens around cations increases as the solvent contains more acetonitrile, implying that adding acetonitrile enhances the interaction between cations and anions under a fixed salt concentration. The viscosity η is connected with the shear modulus G_s and the relaxation time of the shear stress τ_s by the Maxwell relation[32]

$$\eta = G_s \tau_s \quad (1)$$

https://doi.org/10.1021/acs.chemmater.3c01148
Chem. Mater. 2023, 35, 6415−6422

where G_s is proportional to the strength of the inter-molecular interactions and τ_s is associated with the lifetime for structural rearrangement, which is the time for particles to escape the cage. It is reasonable to assume that G_s associated with the ionic network is similar in different solvents as they have similar short-range repulsion and dispersion and a similar long-range electrostatic interaction. Therefore, larger $CN_{O(anion)}$ would lead to a longer time for cations to escape the cage formed by oxygens, which directly relates to the structural relaxation time of peak b. As already discussed in our previous study, a close connection was found between the viscosity and relation time of peak b for the LiTFSI aqueous solution.[33] Furthermore, the increase of $CN_{O(anion)}$ with more acetonitrile becomes less drastic as the fluorocarbon chains of the anions are lengthened, which is consistent with our observation in the concentration dependence of transport properties of the LiBNTI solutions. It is possible that the lengthening of the fluorocarbon chains dilutes the effects of dynamical slowdown contributed by the ionic networks. However, further studies are required to confirm this speculation.

CONCLUSIONS

Although Xu and the collaborators have shown that a 21 m aqueous LiTFSI solution can be an excellent choice of a water-based LIB electrolyte, the high concentration and relatively high viscosity are serious problems.[7] Using acetonitrile and water mixtures as solvents, these two problems can be mitigated. Based on the results of this study, we answered the questions proposed in the beginning of this paper as follows: (1) all the three imide-based anions can form anion networks under relatively low concentrations using water and acetonitrile mixtures as the solvent. This may be one of the reasons that compared with LiTFSI aqueous solutions, using lower salts concentrations,[20] the acetonitrile and water mixture solvent shows the electrochemical stability window, which is as large as the 21 m LiTFSI aqueous electrolyte window. This may be one of the reasons that the use of this mixed solvent in LiTFSI electrolytes at a concentration of 5 m showed an electrochemical stability window comparable to that of LiTFSI aqueous electrolytes at a concentration of 21 m.[20] (2) Based on the MD simulation results, we found that there were two length scales of anion solation structures in the mixture solvent systems: (a) peak a (0.1−0.3 $Å^{-1}$) corresponds to the solvation of the anion clusters by bulk water and (b) peak b (0.4−0.6 $Å^{-1}$) corresponds to the solvation of the anions by acetonitrile. (3) The introduction of acetonitrile can form a more rigid ionic network that causes a more drastic dynamical slowdown. We anticipate that our combined experimental and simulation results can provide guiding principles for developing safer and cheaper electrolytes with better electrochemical performance.

METHODS

Sample Preparation. The electrolytes were prepared by dissolving the LiTFSI (>99%, Sigma-Aldrich), LiBETI (>98%, TCI), and LiBNTI (>95%, TCI) in high-purity water whose conductivity is 18.2 MΩ × cm at 25 °C and with acetonitrile (Sigma-Aldrich) and water and acetonitrile mixtures with 1:1 volume ratio. All the salts are used without further purification. All the electrolytes were prepared by molality (mole salt in kg solvent) used by abbreviated concentrations (0.2, 0.5, 1, 3, 5, 10, 7, 10, 15, 20, and 26).

Small-Angle X-ray Scattering. SAXS experiments were measured at the Advanced Photon Source (APS) 12ID-B and C station of Argonne National Laboratory. The 2D SAXS data were collected on an EIGER2 S detector (DECTRIS Ltd.) with an incident energy of 12 keV. The two-dimensional scattering images were radially averaged over all orientations to produce plots of scattered intensity $I(q)$ versus scattering vector q, where $q = 4\pi \sin \theta/\lambda$. The scattering vector, q, was calibrated using silver behenate. The samples were loaded into 2 mm diameter quartz capillary tubes and sealed with epoxy for the SAXS measurement.

Viscosity. The viscosity of the samples was measured at 25 °C. The viscosity was determined using a μVISC viscometer (RheoSense, Inc.).

MD Simulations. Similar to our previous study,[9,34] the parameters for the anions, cations, and water are taken from[35]L&P,[36]PLS-AA, and[37]PC/E models, respectively. Figure S8 shows the plots of the partial charges from CL&P, Ref X, and Ref X. The CL&P partial charges scaled with a factor of 0.9 seem to be closer to the charges from Zhang et al.,[10] which yielded a good agreement with the X-ray scattering experiment in LiTFSI−water solutions. On the other hand, CL&P partial charges scaled with a factor of 0.8 seem to be closer to the charges from Li et al.,[34] which served as accurate models of both the structures and dynamics of LiTFSI−acetonitrile solutions. Therefore, the charges of anions and cations were scaled by a factor of 0.9 for water and 0.8 for acetonitrile systems, respectively. For the mixture solvent systems, we tested the SAXS profiles using the partial charges with both 0.8 and 0.9 scaling factors, as shown in Figure S9. We found that a scaling factor of 0.9 gives a slightly better estimation of peak a intensity and position for both mixture solvent systems and aqueous solutions. Therefore, we applied 0.9 scaling factor on the partial charges for mixture solvent solutions. Packmol was used to place molecules randomly in the simulation box, and Moltemplate was used to prepare for the topology of the molecules. A large-scale atomic/molecular massively parallel simulator was used to run the MD simulation.[38] We listed the size of the simulation boxes for each system in Table S1. For all systems in this study, we maintained the temperature at 400 K for 200 ps before a 100 ps quenching step to 300 K. We ran an isothermal-isobaric (*NPT*) ensemble for 2 ns and took the average box size from the second half of the *NPT* trajectories. Finally, we obtained 40 ns of production trajectories with the *NVT* ensemble. The time step was set to 2 fs, and a Nosé−Hoover thermostat was used. LiquidLib was used to compute the simulated SAXS profiles and diffusion coefficients.[39] The MD snapshots were visualized using VMD.[40]

ASSOCIATED CONTENT

Supporting Information

The Supporting Information is available free of charge at https://pubs.acs.org/doi/10.1021/acs.chemmater.3c01148.

Characterization data for the materials used in the main text and details are also given regarding MD simulation experiments that were used to verify the assignments of the spectra (PDF)

AUTHOR INFORMATION

Corresponding Authors

Y Z − *Department of Nuclear, Plasma and Radiological Engineering, Beckman Institute for Advanced Science and Technology, and Department of Electrical and Computer Engineering, University of Illinois at Urbana-Champaign, Urbana, Illinois 61801, United States; Joint Center for Energy Storage Research, Argonne National Laboratory, Lemont, Illinois 60439, United States; Department of Nuclear Engineering and Radiological Sciences, University of Michigan, Ann Arbor, Michigan 48109, United States; Department of Materials Science and Engineering, University of Michigan, Ann Arbor, Michigan 48109, United States;* orcid.org/0000-0002-7339-8342; Email: zhyang@illinois.edu

https://doi.org/10.1021/acs.chemmater.3c01148
Chem. Mater. 2023, 35, 6415−6422

Tao Li − *Department of Chemistry and Biochemistry, Northern Illinois University, DeKalb, Illinois 60115, United States; X-ray Science Division, Argonne National Laboratory, Lemont, Illinois 60439, United States; Joint Center for Energy Storage Research, Argonne National Laboratory, Lemont, Illinois 60439, United States;* orcid.org/0000-0002-4913-4486; Email: tli4@niu.edu

Authors

Xinyi Liu − *Department of Chemistry and Biochemistry, Northern Illinois University, DeKalb, Illinois 60115, United States;* orcid.org/0000-0001-6092-2558

Shao-Chun Lee − *Department of Nuclear, Plasma and Radiological Engineering and Beckman Institute for Advanced Science and Technology, University of Illinois at Urbana-Champaign, Urbana, Illinois 61801, United States;* orcid.org/0000-0002-0665-5337

Soenke Seifert − *X-ray Science Division, Argonne National Laboratory, Lemont, Illinois 60439, United States*

Randall E. Winans − *X-ray Science Division, Argonne National Laboratory, Lemont, Illinois 60439, United States; Joint Center for Energy Storage Research, Argonne National Laboratory, Lemont, Illinois 60439, United States;* orcid.org/0000-0002-7080-7673

Complete contact information is available at: https://pubs.acs.org/10.1021/acs.chemmater.3c01148

Author Contributions

Xinyi Liu and Shao-Chun Lee contributed equally to this work. Xinyi Liu prepared and characterized LiTFSI/H_2O, LiTFSI/ACN, and LiTFSI/ACN/H_2O samples under the direction of Tao Li. Theoretical calculations were performed by Shao-Chun Lee and directed by Y Z. Soenke Seifert helped measure the samples with SAXS. The manuscript was composed by Xinyi Li, Shao-Chun Lee, Randall E. Winans, Y Z, and Tao Li.

Notes

The authors declare no competing financial interest.

The authors declare that the data supporting the findings of this study are available within the paper and its Supporting Information files.

■ ACKNOWLEDGMENTS

This work was supported as part of the Joint Center for Energy Storage Research, an Energy Innovation Hub funded by the U.S. Department of Energy, Office of Science, Basic Energy Sciences. This research used resources of the Advanced Photon Source, a U.S. Department of Energy (DOE) Office of Science User Facility operated for the DOE Office of Science by the Argonne National Laboratory under contract no. AC02-06CH11357. T. Li is thankful for the support by the U.S. National Science Foundation (grant nos. 2208972 and 2120559). Y.Z. also acknowledges the U.S. Department of Energy, Office of Science, Office of Basic Energy Sciences, Materials Sciences and Engineering Division, for its continuous support of the development of LiquidLib under award number DE-SC0014084.

■ REFERENCES

(1) Yamada, Y.; Furukawa, K.; Sodeyama, K.; Kikuchi, K.; Yaegashi, M.; Tateyama, Y.; Yamada, A. Unusual stability of acetonitrile-based superconcentrated electrolytes for fast-charging lithium-ion batteries. *J. Am. Chem. Soc.* **2014**, *136*, 5039−5046.

(2) Wang, J.; Yamada, Y.; Sodeyama, K.; Chiang, C. H.; Tateyama, Y.; Yamada, A. Superconcentrated electrolytes for a high-voltage lithium-ion battery. *Nat. Commun.* **2016**, *7*, 1063.

(3) Suo, L.; Oh, D.; Lin, Y.; Zhuo, Z.; Borodin, O.; Gao, T.; Wang, F.; Kushima, A.; Wang, Z.; Kim, H. C.; et al. How Solid-Electrolyte Interphase Forms in Aqueous Electrolytes. *J. Am. Chem. Soc.* **2017**, *139*, 18670−18680.

(4) Qian, J.; Henderson, W. A.; Xu, W.; Bhattacharya, P.; Engelhard, M. H.; Borodin, O.; Zhang, J. G. High rate and stable cycling of lithium metal anode. *Nat. Commun.* **2015**, *6*, 1155.

(5) Yamada, Y.; Wang, J.; Ko, S.; Watanabe, E.; Yamada, A. Advances and issues in developing salt-concentrated battery electrolytes. *Nat. Energy* **2019**, *4*, 269−280.

(6) Yamada, Y.; Yamada, A. Review—Superconcentrated Electrolytes for Lithium Batteries. *J. Electrochem. Soc.* **2015**, *162*, A2406−A2423.

(7) Suo, L.; Borodin, O.; Gao, T.; Olguin, M.; Ho, J.; Fan, X.; Luo, C.; Wang, C.; Xu, K. Water-in-salt electrolyte enables high-voltage aqueous lithium-ion chemistries. *Science* **2015**, *350*, 938−943.

(8) Liu, X.; Yu, Z.; Sarnello, E.; Qian, K.; Seifert, S.; Winans, R. E.; Cheng, L.; Li, T. Microscopic Understanding of the Ionic Networks of "Water-in-Salt" Electrolytes. *Energy Mater. Adv.* **2021**, *2021*, 7368420.

(9) Liu, X.; Lee, S. C.; Seifer, S.; Winans, R. E.; Cheng, L.; Z, Y.; Li, T. Insight into the nanostructure of "water in salt" solutions: A SAXS/WAXS study on imide-based lithium salts aqueous solutions. *Energy Storage Mater.* **2022**, *45*, 696−703.

(10) Zhang, Y.; Lewis, N. H. C.; Mars, J.; Wan, G.; Weadock, N. J.; Takacs, C. J.; Lukatskaya, M. R.; Steinrück, H. G.; Toney, M. F.; Tokmakoff, A.; et al. Water-in-Salt LiTFSI Aqueous Electrolytes. 1. Liquid Structure from Combined Molecular Dynamics Simulation and Experimental Studies. *J. Phys. Chem. B* **2021**, *125*, 4501−4513.

(11) Qian, K.; Winans, R. E.; Li, T. Insights into the Nanostructure, Solvation, and Dynamics of Liquid Electrolytes through Small-Angle X-Ray Scattering. *Adv. Energy Mater.* **2020**, *11*, 2002821.

(12) McEldrew, M.; Goodwin, Z. A. H.; Bi, S.; Kornyshev, A. A.; Bazant, M. Z. Ion Clusters and Networks in Water-in-Salt Electrolytes. *J. Electrochem. Soc.* **2021**, *168*, 050514.

(13) Xiong, T.; Tan, T. L.; Lu, L.; Lee, W. S. V.; Xue, J. Harmonizing Energy and Power Density toward 2.7 V Asymmetric Aqueous Supercapacitor. *Adv. Energy Mater.* **2018**, *8*, 1702630.

(14) Yu, M.; Lu, Y.; Zheng, H.; Lu, X. New Insights into the Operating Voltage of Aqueous Supercapacitors. *Chemistry* **2018**, *24*, 3639−3649.

(15) Wang, X.; Zhou, H.; Sheridan, E.; Walmsley, J. C.; Ren, D.; Chen, D. Geometrically confined favourable ion packing for high gravimetric capacitance in carbon−ionic liquid supercapacitors. *Energy Environ. Sci.* **2016**, *9*, 232−239.

(16) Wang, R.; Liu, P.; Lang, J.; Zhang, L.; Yan, X. Coupling effect between ultra-small Mn 3 O 4 nanoparticles and porous carbon microrods for hybrid supercapacitors. *Energy Storage Mater.* **2017**, *6*, 53−60.

(17) Taggougui, M.; Diaw, M.; Carré, B.; Willmann, P.; Lemordant, D. Solvents in salt electrolyte: Benefits and possible use as electrolyte for lithium-ion battery. *Electrochim. Acta* **2008**, *53*, 5496−5502.

(18) Zhang, Y.; Maginn, E. J. Water-In-Salt LiTFSI Aqueous Electrolytes (2): Transport Properties and Li(+) Dynamics Based on Molecular Dynamics Simulations. *J. Phys. Chem. B* **2021**, *125*, 13246−13254.

(19) Kim, J.; Koo, B.; Lim, J.; Jeon, J.; Lim, C.; Lee, H.; Kwak, K.; Cho, M. Dynamic Water Promotes Lithium-Ion Transport in Superconcentrated and Eutectic Aqueous Electrolytes. *ACS Energy Lett.* **2021**, *7*, 189−196.

(20) Dou, Q.; Lei, S.; Wang, D. W.; Zhang, Q.; Xiao, D.; Guo, H.; Wang, A.; Yang, H.; Li, Y.; Shi, S.; et al. Safe and high-rate supercapacitors based on an "acetonitrile/water in salt" hybrid electrolyte. *Energy Environ. Sci.* **2018**, *11*, 3212−3219.

(21) Borodin, O.; Suo, L.; Gobet, M.; Ren, X.; Wang, F.; Faraone, A.; Peng, J.; Olguin, M.; Schroeder, M.; Ding, M. S.; et al. Liquid

Structure with Nano-Heterogeneity Promotes Cationic Transport in Concentrated Electrolytes. *ACS Nano* **2017**, *11*, 10462−10471.
(22) Lundin, F.; Aguilera, L.; Hansen, H. W.; Lages, S.; Labrador, A.; Niss, K.; Frick, B.; Matic, A. Structure and dynamics of highly concentrated LiTFSI/acetonitrile electrolytes. *Phys. Chem. Chem. Phys.* **2021**, *23*, 13819−13826.
(23) Inoue, P.; Fileti, E.; Malaspina, T. Computational Study of the Properties of Acetonitrile/Water-in-Salt Hybrid Electrolytes as Electrolytes for Supercapacitors. *J. Phys. Chem. B* **2020**, *124*, 5685−5695.
(24) Jeon, J.; Lee, H.; Choi, J.-H.; Cho, M. Modeling and Simulation of Concentrated Aqueous Solutions of LiTFSI for Battery Applications. *J. Phys. Chem. C* **2020**, *124*, 11790−11799.
(25) Popov, I.; Sacci, R. L.; Sanders, N. C.; Matsumoto, R. A.; Thompson, M. W.; Osti, N. C.; Kobayashi, T.; Tyagi, M.; Mamontov, E.; Pruski, M.; et al. Critical Role of Anion−Solvent Interactions for Dynamics of Solvent-in-Salt Solutions. *J. Phys. Chem. C* **2020**, *124*, 8457−8466.
(26) Liu, K.; Li, X.; Cai, J.; Yang, Z.; Chen, Z.; Key, B.; Zhang, Z.; Dzwiniel, T. L.; Liao, C. Design of High-Voltage Stable Hybrid Electrolyte with an Ultrahigh Li Transference Number. *ACS Energy Lett.* **2021**, *6*, 1315−1323.
(27) Yu, Z.; Curtiss, L. A.; Winans, R. E.; Zhang, Y.; Li, T.; Cheng, L. Asymmetric Composition of Ionic Aggregates and the Origin of High Correlated Transference Number in Water-in-Salt Electrolytes. *J. Phys. Chem. Lett.* **2020**, *11*, 1276−1281.
(28) Yu, Z.; Balsara, N. P.; Borodin, O.; Gewirth, A. A.; Hahn, N. T.; Maginn, E. J.; Persson, K. A.; Srinivasan, V.; Toney, M. F.; Xu, K.; et al. Beyond Local Solvation Structure: Nanometric Aggregates in Battery Electrolytes and Their Effect on Electrolyte Properties. *ACS Energy Lett.* **2021**, *7*, 461−470.
(29) Mendez-Morales, T.; Li, Z.; Salanne, M. Computational Screening of the Physical Properties of Water-in-Salt Electrolytes. *Batteries Supercaps* **2020**, *4*, 646−652.
(30) Nilsson, V.; Bernin, D.; Brandell, D.; Edstrom, K.; Johansson, P. Interactions and Transport in Highly Concentrated LiTFSI-based Electrolytes. *Chemphyschem* **2020**, *21*, 1166−1176.
(31) Martins, M. L.; Sacci, R. L.; Lin, X.; Matsumoto, R.; Popov, I.; Cui, J.; Kobayashi, T.; Tyagi, M.; Guo, W.; Dai, S.; et al. Beyond Simple Dilution: Superior Conductivities from Cosolvation of Acetonitrile/LiTFSI Concentrated Solution with Acetone. *J. Phys. Chem. C* **2022**, *126*, 2788−2796.
(32) Rötger, H. Relaxation times and viscosity. *J. Non-Cryst. Solids* **1974**, *14*, 201−217.
(33) Liu, X.; Lee, S. C.; Seifert, S.; He, L.; Do, C.; Winans, R. E.; Kwon, G.; Z, Y.; Li, T. Revealing the Correlation between the Solvation Structures and the Transport Properties of Water-in-Salt Electrolytes. *Chem. Mater.* **2023**, *35*, 2088−2094.
(34) Li, Z.; Robertson, L. A.; Shkrob, I. A.; Smith, K. C.; Cheng, L.; Zhang, L.; Moore, J. S.; Z, Y. Realistic Ion Dynamics through Charge Renormalization in Nonaqueous Electrolytes. *J. Phys. Chem. B* **2020**, *124*, 3214−3220.
(35) Lopes, J. N. C.; Pádua, A. A. H. CL&P: A generic and systematic force field for ionic liquids modeling. *Theor. Chem. Acc.* **2012**, *131*, 1129.
(36) Jorgensen, W. L.; Maxwell, D. S.; Tirado-Rives, J. Development and Testing of the OPLS All-Atom Force Field on Conformational Energetics and Properties of Organic Liquids. *J. Am. Chem. Soc.* **1996**, *118*, 11225.
(37) Berendsen, H. J. C.; Grigera, J. R.; Straatsma, T. P. The Missing Term in Effective Pair Potentials. *J. Phys. Chem.* **1987**, *118*, 6269.
(38) Plimpton, S. Fast Parallel Algorithms for Short-Range Molecular Dynamics. *J. Comput. Phys.* **1995**, *117*, 1−19.
(39) Walter, N. P.; Jaiswal, A.; Cai, Z.; Zhang, Y. LiquidLib: A comprehensive toolbox for analyzing classical and ab initio molecular dynamics simulations of liquids and liquid-like matter with applications to neutron scattering experiments. *Comput. Phys. Commun.* **2018**, *228*, 209−218.
(40) Humphrey, W.; Dalke, A.; Schulten, K. VMD: Visual molecular dynamics. *J. Mol. Graph.* **1996**, *14*, 33−38.

https://doi.org/10.1021/acs.chemmater.3c01148
Chem. Mater. 2023, 35, 6415−6422